九州大学学術情報リポジトリ
Kyushu University Institutional Repository

Activated Factor X Inhibition Ameliorates NF-κB-IL-6–Mediated Perivascular Inflammation and Pulmonary Hypertension

今給黎, 智美

https://hdl.handle.net/2324/7443305

出版情報：Kyushu University, 2025, 博士（医学）, 課程博士
バージョン：
権利関係：© 2025 The Authors.

KYUSHU UNIVERSITY

AMERICAN JOURNAL OF PHYSIOLOGY
LUNG CELLULAR AND MOLECULAR PHYSIOLOGY

Am J Physiol Lung Cell Mol Physiol 329: L183–L196, 2025.
First published June 14, 2025; doi:10.1152/ajplung.00303.2024

RESEARCH ARTICLE

Activated factor X inhibition ameliorates NF-κB-IL-6-mediated perivascular inflammation and pulmonary hypertension

Satomi Imakiire,[1,2] Keiji Kimuro,[1,2] Keimei Yoshida,[1,2]* Kohei Masaki,[1,2] Ryo Izumi,[1,2] Misaki Imabayashi,[1,2] Takanori Watanabe,[1,2] Tomohito Ishikawa,[1,2] Kazuya Hosokawa,[1,2] Shouji Matsushima,[1,2] Toru Hashimoto,[1,2] Keisuke Shinohara,[1,2] Shunsuke Katsuki,[1,2] Tetsuya Matoba,[1,2] Kazufumi Nakamura,[3] Katsuya Hirano,[4] Hiroyuki Tsutsui,[1,2,5] and Kohtaro Abe[1,2]*

[1]Department of Cardiovascular Medicine, Faculty of Medical Sciences, Kyushu University, Fukuoka, Japan; [2]Division of Cardiovascular Medicine, Faculty of Medical Sciences, Research Institute of Angiocardiology, Kyushu University, Fukuoka, Japan; [3]Department of Cardiovascular Medicine, Okayama University, Okayama, Japan; [4]Department of Cardiovascular Physiology, Faculty of Medicine, Kagawa University, Takamatsu, Japan; and [5]School of Medicine and Graduate School, International University of Health and Welfare, Okawa, Japan

Abstract

Activated factor X (FXa) induces inflammatory response and cell proliferation in various cell types via activation of proteinase-activated receptor-1 (PAR_1) and/or PAR_2. We thus aimed to investigate the impact of FXa on the development of pulmonary arterial hypertension (PAH) and the mechanisms involved. The effects of edoxaban, a selective FXa inhibitor, on hemodynamic, right ventricular (RV) hypertrophy, and vascular remodeling were evaluated in a monocrotaline (MCT)-exposed pulmonary hypertension (PH) rat model. At 21 days after a single subcutaneous injection of MCT of 60 mg/kg, right ventricular systolic pressure (RVSP) and total pulmonary vascular resistance index (TPRI) were elevated concomitant with the increased plasma FXa and lung interleukin-6 (*IL-6*) mRNA. Daily administration of edoxaban (10 mg/kg/day, by gavage) starting from the day of MCT injection for 21 days ameliorated RVSP, TPRI, RV hypertrophy, pulmonary vascular remodeling, and macrophage accumulation. Edoxaban reduced nuclear factor-kappa B (NF-κB) activity and *IL-6* mRNA level in the lungs of MCT-exposed rats. mRNA levels of *FXa*, *PAR_1*, and *PAR_2* in cultured pulmonary arterial smooth muscle cells (PASMCs) isolated from patients with PAH were higher than those seen in normal PASMCs. FXa stimulation increased cell proliferation and mRNA level of *IL-6* in normal PASMCs, both of which were blunted by edoxaban and PAR_1 antagonist. Moreover, FXa stimulation activated extracellularly regulated kinases 1/2 in a PAR_1-dependent manner. Inhibition of FXa ameliorates NF-κB-IL-6-mediated perivascular inflammation, pulmonary vascular remodeling, and the development of PH in MCT-exposed rats, suggesting that FXa may be a potential target for the treatment of PAH.

NEW & NOTEWORTHY This study demonstrated that chronic treatment with activated factor X (FXa) inhibitor ameliorated NF-κB-IL-6-mediated perivascular inflammation in a rat model with pulmonary arterial hypertension, which is associated with elevated FXa activity. FXa may act on pulmonary arterial smooth muscle cells, inducing cell proliferation and inflammatory response via upregulated PAR_1, thereby contributing to pulmonary vascular remodeling. Understanding the patient-specific pathophysiology is a prerequisite for applying FXa-targeted therapy to the treatment of pulmonary arterial hypertension.

factor Xa; IL-6; proteinase-activated receptor; pulmonary arterial hypertension; pulmonary hypertension

INTRODUCTION

Pulmonary arterial hypertension (PAH) is characterized by progressive increases in pulmonary vascular resistance (PVR) and pulmonary arterial pressure (PAP), leading to right ventricular (RV) failure (1). Pulmonary vasodilators, including prostacyclin and its analogues, soluble guanylate cyclase stimulator, phosphodiesterase type 5 inhibitors, and endothelin receptor antagonists, have successfully delayed clinical deterioration of PAH and improved survival (2). However, the prognosis of advanced cases remains poor. Therefore, a better understanding of the pathogenesis of PAH and the development of novel therapeutic strategies is needed.

The pathology of PAH involves multiple factors such as enhanced vasoconstriction, vascular remodeling, and in situ thrombosis of small pulmonary arteries and arterioles, all of which act interactively, contributing to increase PVR and PAP (3). In particular, thrombotic lesions and thrombotic arteriopathy are common pathological findings in PAH (4).

*K. Yoshida and K. Abe contributed equally to this work.

Correspondence: K. Yoshida (yoshida.keimei.713@m.kyushu-u.ac.jp); K. Abe (abe.kotaro.232@m.kyushu-u.ac.jp).

Submitted 17 September 2024 / Revised 30 October 2024 / Accepted 31 May 2025

1040-0605/25 Copyright © 2025 The Authors. Licensed under Creative Commons Attribution CC-BY-NC-ND 4.0.
Published by the American Physiological Society.

Downloaded from journals.physiology.org/journal/ajplung (124.247.150.004) on July 27, 2025.

Vascular lesions exhibit increased expression of tissue factor (5). Tissue factor forms a complex with circulating factor VIIa (FVIIa), and the tissue factor/FVIIa complex subsequently converts factor X (FX) to activated factor X (FXa), which then catalyzes the generation of thrombin. Association of high blood coagulability and PAH has been proposed in several studies (6–8), one of which showing increased plasma level of endogenous thrombin potential in patients with PAH (9). Although increased coagulability contributes to formation of in situ thrombosis, it could also contribute to vascular remodeling since FXa, thrombin and other coagulation factors with proteinase activity are known to activate proteinase-activated receptor-1 (PAR_1) and/or PAR_2 which exert coagulation-independent effects including perivascular inflammation and cell proliferation in various cell types (10, 11). We and other groups have demonstrated that PAR_1 and PAR_2 antagonists attenuate pulmonary vascular remodeling and improve experimental pulmonary hypertension (PH) (12, 13). Thus, the coagulation-independent effects of coagulation factors may play an important role in the development and progression of PAH. However, the upstream factors that activate PAR_1 or PAR_2 in PAH remain unknown. Moreover, the effect of edoxaban, known as a direct FXa inhibitor, in PAH pulmonary vasculature and interaction with PAR_1/PAR_2 remains unveiled.

In the present study, we hypothesized that FXa may exacerbate perivascular inflammation and cell proliferation, leading to pulmonary vascular remodeling and the development of PAH. To test our hypothesis, we evaluated the plasma levels of FXa in monocrotaline (MCT)-exposed experimental PH model rats. We then examined whether chronic inhibition of FXa attenuates the pathology of experimental PH with respect to hemodynamic, inflammatory response, and vascular remodeling in the PH rat model. We used edoxaban, which binds directly to FXa and inhibits its activity, for chronic inhibition of FXa. We also used cultured human pulmonary arterial smooth muscle cells (PASMCs) to test whether FXa stimulation induces an inflammatory response and cell proliferation, and whether PAR_1 or PAR_2 is involved in these pathways.

MATERIALS AND METHODS

Animal Experiments

All animal procedures were performed in compliance with the principles of the NIH Guide for the Care and Use of Laboratory Animals as well as Kyushu University Animal Experiment Regulations (129th Edition, 2021). All experimental protocol was approved (Approval No.: A20-219-0) by the Institutional Animal Care and Use Committee of Kyushu University, Japan.

Drugs

Monocrotaline (MCT; Sigma-Aldrich, Saint Louis, MO) was dissolved in 1 N HCl, neutralized with 1 N NaOH, and diluted with distilled water to 20 mg/mL. SU5614 (Tocris, Bristol) was dissolved in carboxymethyl cellulose solution to 4 mg/mL. Edoxaban provided by Daiichi Sankyo Co. Ltd. (Tokyo, Japan) was dissolved in 0.5% methylcellulose at 1 mg/mL for in vivo studies and in dimethyl sulfoxide (DMSO) at 10 mM for in vitro studies. Human FXa purchased from Hematologic Technologies (Cat. No. HCXA-0060, New York), a PAR_1 antagonist (E5555, Cat. No. 2030, Adipo-Gen, San Diego), and a PAR_2 antagonist (FSLLRY-NH_2, Cat. No. 4751, Bio-Techne, Minneapolis) were dissolved in DMSO at 50 nM, 1 μM, and 50 μM, respectively. Edoxaban, FXa, E5555, and FSLLRY-NH_2 were further diluted in Dulbecco modified Eagle's medium (DMEM; Cat. No. 05915, Nissui, Japan) for in vitro studies.

Experimental Protocols for Monocrotaline-Exposed Rat Model

Adult male Sprague–Dawley 5–6 wk old rats weighing 200–250 g (Japan SLC, Hamamatsu, Japan) were allocated to the following four groups; *1*) age-matched normal rats (normal), *2*) MCT alone, *3*) MCT with low dose of edoxaban (3 mg/kg/day), and *4*) MCT with high dose of edoxaban (10 mg/kg/day). Normal rats were given a subcutaneous injection of phosphate-buffered saline (PBS). Rats in the MCT group were given a single subcutaneous injection of MCT at 60 mg/kg (14). Edoxaban was administered daily by gavage from the day of MCT injection (*day 0*) to *day 21*. Normal rats were administered a solvent solution (0.5% methylcellulose) without edoxaban daily by gavage. In addition, we have performed a reversal protocol of high-dose edoxaban (10 mg/kg/day) from *day 14* after MCT injection to *day 24*. We used male rats because a previous report showed a more aggressive course of MCT-exposed PH in males compared with females (15). A total of 72 rats were used for hemodynamic, histology, and immunohistochemistry studies, 28 rats for reverse transcription-polymerase chain reaction (RT-PCR) and Western blot analyses, and 22 rats for FXa activity test.

FXa Activity Assay

Plasma FXa activity was measured using substrate S-2765 (Cat. No. 214608, Chromogenix, Milano, Italy), as described previously (16, 17). Briefly, 100 μL of rat plasma was mixed with 100 μL of 1.25 mg/mL S-2765 at 37°C. Absorbance at 405 nm was read on a spectrophotometer every 5 min up to 30 min. The activity of FXa was derived by comparing the initial rate (ΔA/min) against the FXa standard curve.

Hemodynamic Evaluation in Rats

Hemodynamic parameters were evaluated as described previously (18, 19). Briefly, a rat was anesthetized with isoflurane (initiated at 3%, maintained at 1.5% in room air). An 18-gauge BD Angiocath catheter (Becton Dickinson) with the tip at a 30° angle, which was connected to a fluid filled transducer (DX-360, Nihon Kohden, Japan), was inserted into the right jugular vein and advanced into the right ventricle (RV) for measurement of RV systolic pressure (RVSP) (20). A microtip P-V catheter (FTH-1912B8018, Transonic Inc., Ithaca, NY) was inserted into the right carotid artery and then advanced into the left ventricle (LV). The RVSP, left ventricle systolic pressure (LVSP), heart rate (HR), and cardiac output (CO) were continuously recorded using ML880/9 Power Lab 16/30 (AD Instruments, Dunedin, New Zealand), an advantage P-V control unit (v 5.0) (FY097B, Transonic

Downloaded from journals.physiology.org/journal/ajplung (124.247.150.004) on July 27, 2025.

Inc.) and a dedicated laboratory computer system. Cardiac index (CI) was calculated by dividing CO by the body weight. The ratio of RVSP to CI (RVSP/CI) yielded a surrogate marker of total pulmonary vascular resistance index (TPRI). After catheterization, the rat was euthanized by exsanguination under an overdose of isoflurane (2%–5% in room air) and intraperitoneal injection of a lethal dose of pentobarbital sodium. The heart was removed for assessment of RV hypertrophy (RVH), and the lungs were collected for histological evaluation, immunoblot analysis, and RT-PCR. The tissues for control and treatment groups were collected at the same time under the same conditions. RVH was evaluated using a ratio of the RV weight to the weight of the left ventricle plus septum [RV/(LV + S)].

Histopathological Analysis

The left lobe of each lung was isolated and inflated with PBS containing 1% formalin and 0.5% agarose via the trachea at a constant pressure of 20 cmH_2O, and was then fixed in 10% formalin neutral buffer solution overnight. After embedding in paraffin, 5-μm-thick slices obtained at the level of the hilum were subjected to Elastin van Gieson (EVG) staining and immunohistochemical staining (18).

Medial wall thickness.

Small pulmonary arteries with outer diameters from 50 to 100 μm were analyzed (21, 22). The medial wall thickness (MWT) index was obtained using the following formula: MWT = (outer diameter − inner diameter)/outer diameter. Outer and inner diameters are based on the circumferences of the outer and inner elastic laminae, respectively. At least 10 arteries were analyzed, and the mean MWT was obtained for each animal. The analysis was performed in a blinded manner.

Muscularization of small pulmonary arteries.

Pulmonary arteries with outer diameters of 50 μm or less were analyzed (13). Nonmuscularized (NM), partially muscularized (PM), and fully muscularized (FM) arterioles were defined as positive staining of α-smooth muscle actin in < 25%, 25%–75%, and > 75%, respectively, of the circumference of the arteriole. At least 70 arterioles were evaluated for each specimen in a blinded manner.

Immunohistochemical Analysis

Immunohistochemical staining was performed using the Vectastain Universal Quick kit (Vector Laboratories, Newark, CA), as described previously (23). The sections were incubated with primary antibody reactive to α-smooth muscle actin (SMA; 1:500 dilution, Cat. No. M085101, Agilent DAKO, Santa Clara, CA), Ki67 (1:400 dilution, Cat. No. RM-9106, Thermo Scientific K.K., Tokyo, Japan), CD68 (1:100 dilution, Cat. No. ab31630, Abcam, Cambridge, UK), and nuclear factor kappa B (NF-κB; 1:200 dilution, Cat. No. MAB3026, Merck KGaA, Darmstadt, Germany) at 4°C overnight. Sections were then incubated with biotinylated secondary antibody, followed by incubation with horseradish peroxidase-labeled streptavidin. The immune complex was visualized using 3,3′-diaminobenzidine.

Cell proliferation in media of pulmonary arteries.

Proliferative cells were detected by immunostaining with anti-Ki67 antibody (18). The number of Ki67-positive cells in the media of pulmonary arteries in 15 random fields was counted at a magnification of ×400.

Macrophage accumulation.

Macrophages were detected by immunostaining with anti-CD68 antibody (24). The number of CD68-positive macrophages in 15 random fields was counted at a magnification of ×400.

NF-κB activity.

The active form of NF-κB was detected using the anti-p65 monoclonal antibody that recognizes an epitope on the p65 subunit of NF-κB, which is exposed for antibody detection after dissociation by inhibitor of κB (I-κB), i.e., activation of NF-κB (24). An uninformed observer counted the number of NF-κB-positive cells in 20 random fields at a magnification of ×400 (25). NF-κB positive cells were counted in CD68-positive macrophages (extravascular), and endothelial cells and PASMCs (intravascular).

Reverse Transcription-Polymerase Chain Reaction Analysis

Total RNAs were extracted from whole lung and PASMCs using the RNeasy mini kit (Cat. No. 74106, QIAGEN, Hilden, Germany), and mRNA expression level was determined by

Table 1. *Primer sequences for cDNA*

	Forward (5′→3′)	Reverse (5′→3′)
Human primer		
IL-6	GGT ACA TCC TCG ACG GCA TCT	GTG CCT CTT TGC TTT CAC
MCP-1	ATA GCA GCC ACC TTC ATT CC	ATC CTG AAC CCA CTT CTG CT
PAI-1	TGA GAT CAG CAC AGA C	ATT GAT GAA TCT GGC TCT C
FX	GCC CAC TGT CTC TAC CAA GC	CTT GAT GAC CAC CTC CAC CT
PAR_1	CCG CCT GCT TCA GTC TGT G	GGT TCC TGA GAA ATG ACC G
PAR_2	CTT CCA GGA YGC GGA G	TGG GAT GTG CCA TCA ACC TTA
18s	AAG TTT CAG CAC ATC CTG CGA GTA	TTG GTG AGG TCA ATG TCT GCT TTC
Rat primer		
IL-6	ATT GTA TGA ACA GCG ATG CAC	CCA GGT AGA AAC GGA ACT CCA GA
MCP-1	CTC TTC CTC CAC TAT GC	CTC TGT CAT ACT GGT CAC TTC
PAI-1	CTT TAT CCT GGG TCT CCT G	TGA TGC CTC CCT GAC ATA CA

Downloaded from journals.physiology.org/journal/ajplung (124.247.150.004) on July 27, 2025.

RT-PCR (24). The ReverTra Ace qPCR kit (No. FSQ-101, TOYOBO, Tokyo, Japan) and SYBR Premix Ex TaqII (Cat. No. RR820, TaKaRa, Tokyo, Japan) were used for reverse transcription and amplification, respectively. PCR primers and probes were purchased from TaKaRa. A 10-μL RT reaction mixture containing 200 ng of total RNA, oligo dT primer, random primer, and Moloney murine leukaemia virus reverse transcriptase was subjected to transverse transcription. An aliquot of RT product was diluted with water, and 25 ng of the cDNA was subjected to real-time PCR analysis using the 7500 Real-Time PCR System (Applied Biosystems). The thermal cycle consisted of an initial denaturation at 95°C for 30 s, followed by 40 cycles of denaturation at 95°C for 5 s and annealing at 60°C for 34 s. The melt curve of the PCR product was analyzed at the end of the real-time PCR analysis, and a single peak was detected in the melt curve. Agarose gel electrophoresis confirmed that each PCR product showed a single band with the expected molecular size. We used the ΔΔCt method to analyze the fluorescence data using 18S rRNA as an internal control. Table 1 shows the primer sets used in the present study.

Western Blotting

PASMCs are washed with 0.1 mM ethylenediamine tetraacetic acid (EDTA)/phosphate buffered saline (PBS) and then collected by adding radio-immunoprecipitation assay (RIPA), pH 7.5, containing 50 mM Tris-HCl, 150 mM NaCl, 1% (vol/vol) Nonidet P-40, 1% Na-deoxycholate, 0.1% sodium dodecyl sulfate (SDS), 1 mM dithiothreitol, 0.5 mM Na_3VO_4, 10 μg/mL leupeptin, 10 μg/mL aprotinin, 5 μM microcystin-LR, 10 μM calpain inhibitor, and 10 μM 4-aminidophenylmethane sulfonyl fluoride. The collected PASMC were frozen at −80°C and subsequently homogenized. The protein concentration of the lysate was determined using a Coomassie protein assay kit (Cat. No. 23225, Pierce, Rockford, IL) with bovine serum albumin as a standard. Equal amounts of total proteins (10 μg) were separated on 10% (wt/vol) polyacrylamide gels by sodium dodecyl sulfate polyacrylamide gel electrophoresis and transferred to a polyvinylidene difluoride membrane (0.2 μm pore size; Bio-Rad, Hercules, CA) (26). The membranes were blocked with 5% (wt/vol) skim milk in 20 mM Tris-HCl, pH 7.5, containing 150 mM NaCl and 0.05% (vol/vol) Tween 20 (Tween 20-containing Tris-buffered saline) for 1 h at room temperature. The membranes were then incubated overnight at 4°C with primary antibodies against p44/42 extracellularly regulated kinases (ERK) (a marker of ERK1/2; 1:3,000 dilution, Cat. No. 4695, Abcam), phosphorylated p44/42 ERK (1:3,000 dilution, Cat. No. 4370, Abcam), p65 (1:5,000 dilution, Cat. No. 8242, CST), phospho-p65 (1:5,000 dilution, Cat. No. 3033, CST), and glyceraldehyde-3-phosphate dehydrogenase (GAPDH; 1:5,000 dilution, Cat No. 2118, Cell Signaling Technology, Danvers), followed by 1-h incubation with secondary antibodies conjugated to horseradish peroxidase (1:5,000 dilution; Santa Cruz, Dallas) (Supplemental Fig. S1; 27). The immune complexes were detected using an ECL select detection kit (GE Healthcare, Buckinghamshire, UK). Light emission was detected and analyzed with VersaDoc 5000 and the computer program Quantity One (Bio-Rad, CA). The optical densities of ERK and phosphorylated ERK bands were normalized to those of the corresponding GAPDH bands.

Table 2. *Clinical data pf patients*

Patient	Age (Years Old)	Sex	Diagnosis	Gene Mutation	Passage
Normal					
1	67	male	Lung cancer		6
2	58	male	Lung cancer		7
3	54	male	Lung cancer		5
PAH					
1	11	female	HPAH	BMPR2:p, Arg 491	6
2	10	male	IPAH		3
3	11	male	IPAH		9
4	11	male	IPAH		5

HPAH, heritable pulmonary arterial hypertension; IPAH, idiopathic pulmonary arterial hypertension.

Table 3. *Primer sequences for siRNA*

	Forward (5′→3′)	Reverse (5′→3′)
PAR-1	GAG TTG GGA TTG GAC AGT AG	GCT AGG ATT ACA GGC ATG AG

Cell Culture

PASMCs were isolated and established from the lungs of four patients with PAH (PAH-PASMCs) and three patients with bronchogenic carcinoma (normal PASMCs) (Table 2), as reported previously (28). The cells used in this study were provided by Okayama University. All of the studies were approved by the Ethics Committee of Okayama University Graduate School of Medicine, Dentistry, and Pharmaceutical Sciences, and written informed consent was obtained from all patients before the procedure. All cells were provided by Okayama University, and written informed consent was obtained from all patients before the procedure. Cell identification was confirmed by examination of cytoskeletal components, α-smooth muscle

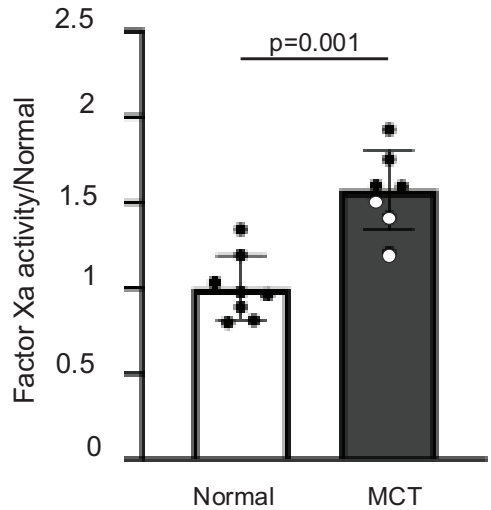


Figure 1. Quantification of factor Xa activity in plasma of normal and monocrotaline-exposed rats. Activated factor X (Factor Xa) activities in the plasma of normal and monocrotaline (MCT)-exposed PH rats were measured by ELISA at *day 21* after MCT injection. Normal: normal rats injected with PBS, MCT: rats injected with MCT. $n = 7$ or 8, analyzed by unpaired *t* test. PBS, phosphate-buffered saline.

Downloaded from journals.physiology.org/journal/ajplung (124.247.150.004) on July 27, 2025.

actin (αSMA), myosin, and smoothelin. The growth medium used was DMEM supplemented with 10% fetal bovine serum (FBS) and 1% penicillin/streptomycin. The cells were incubated in a humidified 5% CO_2 atmosphere at 37°C. The medium was changed every 3 days. Cells between passages 3–10 were used for all experiments.

Cell Proliferation Assays

Cell proliferation was evaluated using a 5-bromo-2'-deoxyuridine (BrdU) cell proliferation kit (Cell Proliferation ELISA, colorimetric, Cat. No. 11647229001; Roche Applied Science, Mannheim, Germany), according to the manufacturer's recommendations (29). In brief, PASMCs at a density of 5,000 cells/cm^2 were seeded in 96-well plates, cultured for 24 h, and then serum-starved for an additional 24 h. Subsequently, the cells were incubated with human FXa (50 nM) with or without E5555 (1 μM), FSLLRY-NH2 (50 μM), or edoxaban (100 nM). BrdU (10 μM) was added at 21 h after FXa stimulation. After 24-h exposure to BrdU, the amount of BrdU incorporation was quantified by ELISA. The data are expressed as fold increase relative to the values obtained from normal PASMCs. The FXa concentration of 50 nM used in the assay is considered to be within the physiologically relevant range (150–200 nM FXa in human plasma) (30). The concentrations of PAR_1 and PAR_2 inhibitors were similar to those used in previous studies on vascular smooth muscle cells (VSMCs) (11, 31). The concentration of edoxaban is considered to be within the clinically relevant range, as edoxaban concentration of 256 nM in human plasma prolonged prothrombin time by twofold (32).

FXa Stimulation in Pulmonary Artery Smooth Muscle Cells

PASMCs at a density of 2.0×10^5 cells were seeded in a 35 mm dish, cultured for 24 h, and then serum-starved for an additional 24 h. Subsequently, the cells were incubated with human FXa (50 nM) with or without E5555 (1 μM), FSLLRY-NH2 (50 μM), or edoxaban (100 nM). After 3 h of incubation, samples for PCR were collected using Buffer RLT in the RNeasy mini kit, and Western blots were collected using RIPA as described earlier.

Transfection of siRNA

Knockdown of PAR-1 gene expression in PASMC was achieved by the small interfering RNA (siRNA) technique. Transfection of cultured PASMC was carried out by Lipofectamine RNAiMAX (Cat. No. 13778100, Thermo Fisher Scientific, Massachusetts) according to the proposed protocol (33). Briefly, Cells were seeded to be 60%–80% confluent at the time of transfection, and both

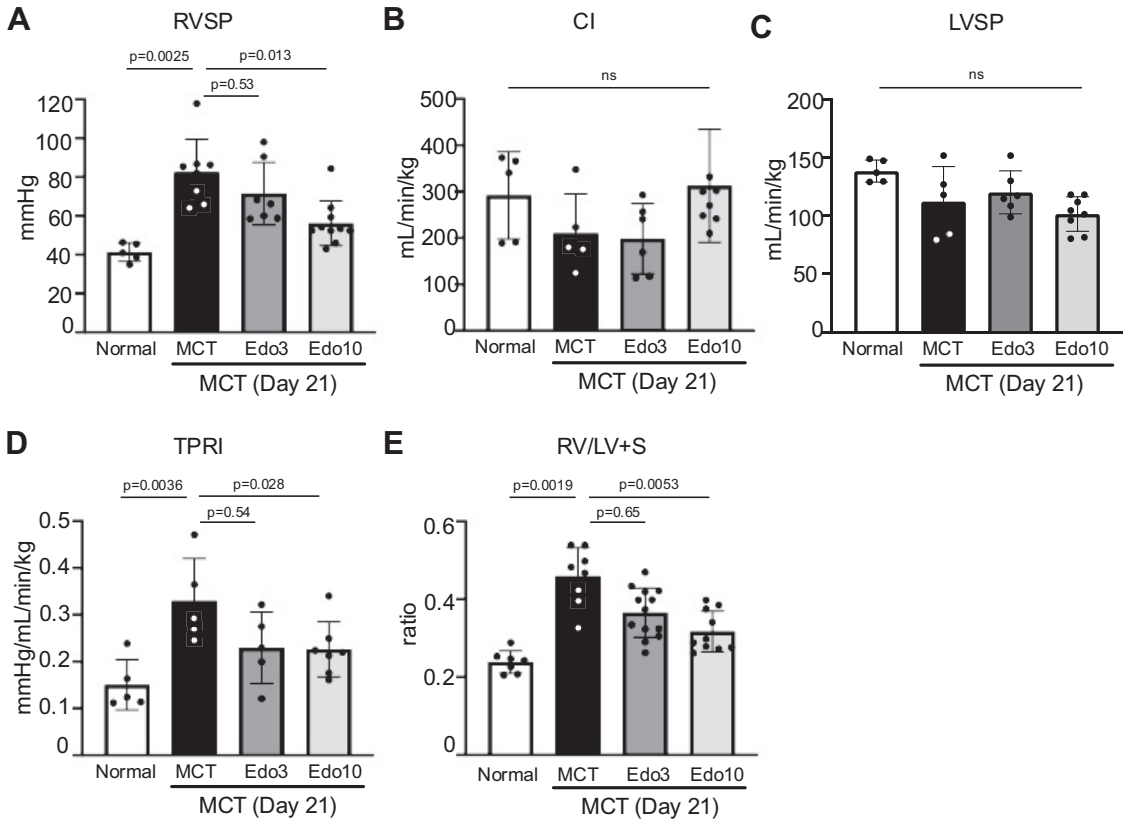


Figure 2. Effects of long-term treatment with edoxaban on hemodynamic parameters and right ventricular hypertrophy in monocrotaline-exposed rats. Rats were given a subcutaneous injection of monocrotaline (MCT) on *day 0*. Some MCT-injected rats were treated with a low dose (3 mg/kg/day; Edo3) or high dose of edoxaban (10 mg/kg/day; Edo10) from *day 0* to *day 21* after MCT injection. Normal: normal rats injected with PBS. Shown are the summaries of right ventricular systolic pressure (RVSP) (*A*), cardiac index (CI) (*B*), left ventricular pressure (LVSP) (*C*), total pulmonary vascular resistance index (TPRI) (*D*), and right ventricular hypertrophy [RV/(LV + S): weight ratio of RV free wall to sum of LV free wall and septum] (*E*). Data are expressed as mean ± SD. $n = 5$–12, analyzed by one-way ANOVA followed by Bonferroni post hoc test. PBS, phosphate-buffered saline.

Downloaded from journals.physiology.org/journal/ajplung (124.247.150.004) on July 27, 2025.

siRNA and Lipofectamine RNAiMAX were dissolved in OptiMEM medium (Cat. No. 31985062, Thermo Fisher Scientific, Massachusetts) and mixed 1:1, added to cells to a concentration of 5 nmol/L and incubated for 24 h. Then cells were used for RT-PCR analysis and FXa stimulation experiments. The sequence of siRNA against PAR-1 is described in Table 3. Successful transfection was verified by Western blotting using cells transfected with noncoding siRNA as a control.

Experimental Protocol for SU5416/Hypoxia/Normoxia-Induced PH Rat

Adult male Sprague–Dawley rats weighing 180–220 g were injected subcutaneously with SU5416 (20 mg/kg) and exposed to hypoxia (10% O_2) for 3 wk (18), followed by returning to normoxia (21% O_2) for an additional 2 wk (total 5 wk after SU5416 injection) to produce PH model rats. Plasma FXa activity was analyzed as described in the MATERIALS AND METHODS section above, *FXa Activity Assay*. Edoxaban (10 mg/kg; by gavage) was administered from the day of SU5416 injection through to the end of *week 5*. Normal rats were administered a solvent solution (0.5% methylcellulose) without edoxaban daily by gavage. The rats were then euthanized as described in MCT-exposed PH model rats for evaluation of hemodynamic parameters and RVH.

Statistical Analysis

Data are expressed as mean ± SD. Student's *t* test was used in two-group comparisons. ANOVA followed by a Bonferroni post hoc test was used in comparisons among multiple experimental groups. Differences were considered significant at $P < 0.05$.

RESULTS

Factor Xa Activity in Monocrotaline-Exposed Rats

Plasma FXa activity in MCT-exposed rats at *day 21* was significantly higher than that in normal rats (Fig. 1).

Long-Term Edoxaban Treatment on Hemodynamic and RV Hypertrophy in Monocrotaline-Exposed Rats

Figure 2 demonstrates the hemodynamic and morphological analysis of long-term edoxaban treatment in MCT-exposed rats. In the MCT group, RVSP and TPRI significantly increased, whereas CI and LVSP showed no remarkable difference compared with those seen in the normal group. The RV/(LV + S) ratio, indicating RVH, also increased significantly in the MCT group compared with the normal group. The mean systemic arterial pressure and heart rate did not differ significantly between the MCT group and the normal group (data not shown). The high dose of edoxaban (10 mg/kg/day) significantly ameliorated the increases in RVSP, TPRI, and RV/LV + S, but had no significant effect on CI in MCT-exposed PH rats. The low dose of edoxaban (3 mg/kg/day) exhibited no significant effects on all the indexes. Both doses of edoxaban had no effects on mean systemic arterial pressure and heart rate (data not shown). Meanwhile, the reversal protocol of high-dose edoxaban from *day 14* after MCT injection to *day 24* did not lower RVSP or RV/LV + S (Supplemental Fig. S2).

Effects of Edoxaban on Pulmonary Vascular Remodeling in Monocrotaline-Exposed Rats

Medial wall hypertrophy in muscular arteries, a manifestation of vascular remodeling in PH, was evaluated in

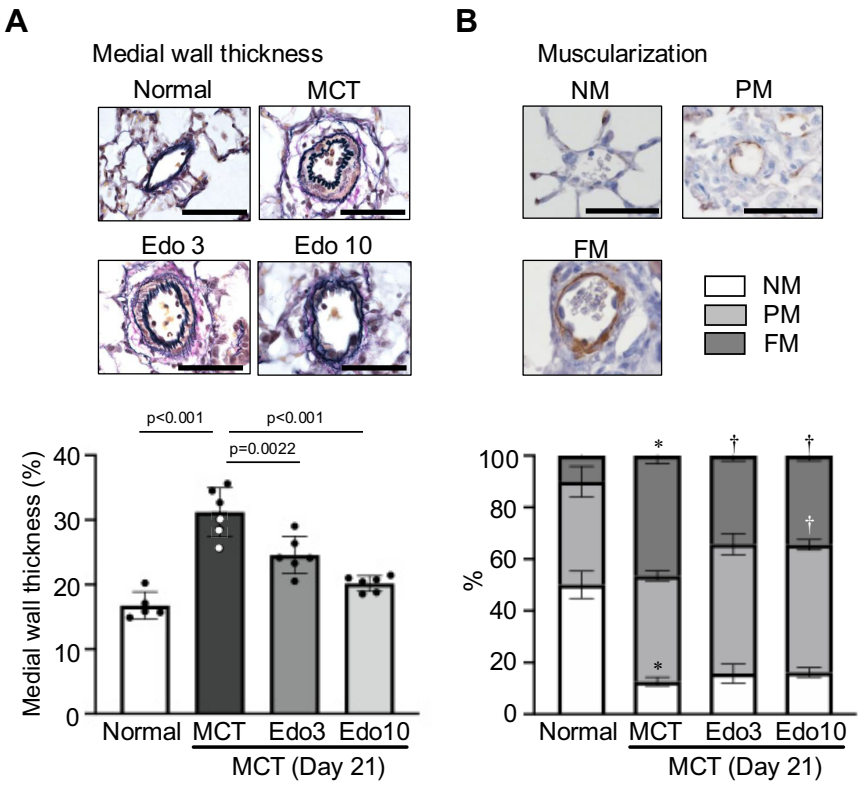


Figure 3. Effects of long-term treatment with edoxaban on pulmonary vascular remodeling in monocrotaline-exposed rats. Rats were given a subcutaneous injection of monocrotaline (MCT) on *day 0*. Some MCT-injected rats were treated with a low dose (3 mg/kg/day; Edo3) or high dose of edoxaban (10 mg/kg/day; Edo10) from *day 0* to *day 21* after MCT injection. Normal: normal rats injected with PBS. *A*: representative photomicrographs of Verhoeff-van Gieson staining and summary of medial wall thickness of pulmonary arteries with outer diameters of 50–100 μm. *B*: representative photomicrographs of immunohistochemical staining of α-smooth muscle actin showing nonmuscularized (NM), partially muscularized (PM), and fully muscularized (FM) patterns, and summary of muscularization in pulmonary arterioles with outer diameters of 50 μm or less. Scale bars are 50 μm each. Data are expressed as mean ± SD. $n = 6$. *B*: *p(FM) =0.033 and *p(NM) = 0.042 vs. Normal; †p(Edo3 FM) = 0.042, †p(Edo10 FM) = 0.039, and †p (Edo10 PM) = 0.04 vs. MCT, analyzed by one-way ANOVA followed by Bonferroni post hoc test. PBS, phosphate-buffered saline.

Downloaded from journals.physiology.org/journal/ajplung (124.247.150.004) on July 27, 2025.

pulmonary arteries with outer diameters ranging from 50 to 100 μm. The medial wall thickness was significantly increased at *day 21* in the MCT group compared with the normal control group (Fig. 3*A*). Administration of low or high dose of edoxaban significantly reduced the thickness of the medial wall of pulmonary arteries compared with untreated MCT-exposed rats (Fig. 3*A*). No parenchymal lung lesions and thrombotic lesion were observed in pulmonary arteries in all groups.

Muscularization of the arterioles, another manifestation of vascular remodeling in PH, was evaluated in arterioles with outer diameters of 50 μm or less. Immunohistochemical detection of α-smooth muscle actin and quantitative evaluation of the degree of positive staining relative to the circumferential length revealed a significant increase in percentage of partially and fully muscularized arterioles in the MCT group at *day 21* after MCT injection compared with normal rats (Fig. 3*B*). Treatment with high dose of edoxaban significantly decreased the fractions of both partially and fully muscularized pulmonary arterioles in MCT-exposed rats, whereas low dose of edoxaban significantly decreased the fraction of only fully muscularized arterioles (Fig. 3*B*).

Effects of Edoxaban on Cell Proliferation and Inflammatory Responses in Monocrotaline-Exposed Rats

The number of Ki67-positive cells, indication of cell proliferation, in the media of muscular arteries significantly increased in the MCT group compared with the normal control group (Fig. 4*A* and Supplemental Fig. S3). Treatment with edoxaban significantly decreased the number of Ki67-positive cells (Fig. 4*A*). Infiltration of CD68-positive macrophages and the number of active NF-κB-positive cells in the areas surrounding small pulmonary arteries significantly

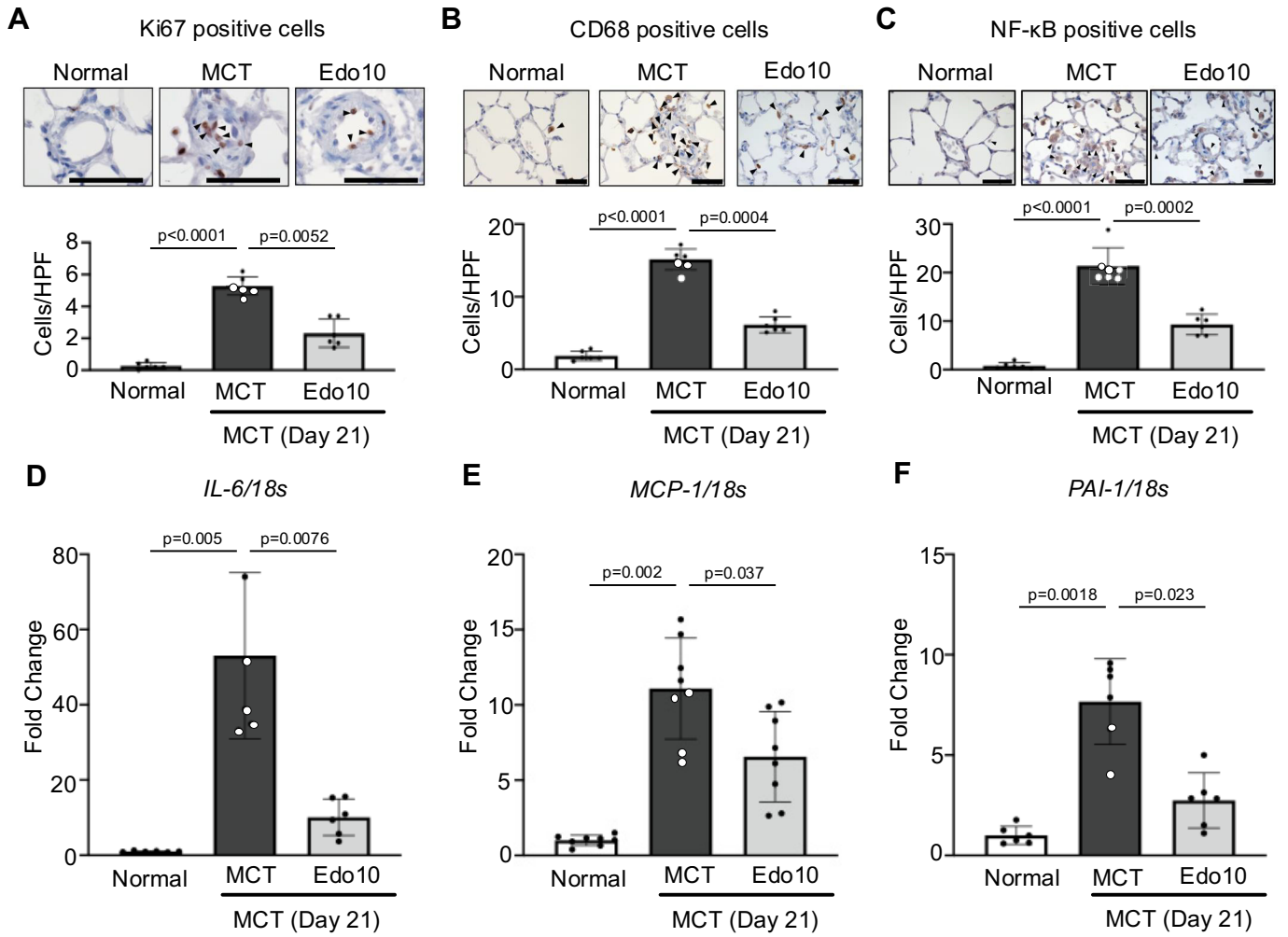


Figure 4. Effects of long-term treatment with edoxaban on proliferation, perivascular inflammation, and inflammatory signaling in monocrotaline-exposed rats. Rats were given a subcutaneous injection of monocrotaline (MCT) on *day 0*. Some MCT-injected rats were treated with edoxaban (10 mg/kg/day; Edo10) from *day 0* to *day 21* after MCT injection. Normal: normal rats injected with PBS. *A*–*C*: representative photomicrographs and summaries of Ki67-positive cells (*A*; arrowheads), CD68-positive macrophages (*B*; arrowheads), and active NF-κB-positive cells (*C*; arrowheads) in medial layer (*A*) and in the surrounding areas (*B* and *C*) of pulmonary arteries with outer diameters of 50 μm or less. Scale bars indicate 50 μm. *D*–*F*: summaries of mRNA expression levels of *Il-6* (*D*), *MCP-1* (*E*), and *PAI-1* (*F*) in lung measured by RT-PCR. Data are expressed as mean ± SD. $n = 6$–8. analyzed by one-way ANOVA followed by Bonferroni post hoc test. Il-6, interleukin-6; MCP-1, macrophage chemoattractant protein-1; PAI-1, plasminogen activator inhibitor-1; PBS, phosphate-buffered saline.

Downloaded from journals.physiology.org/journal/ajplung (124.247.150.004) on July 27, 2025.

increased in the MCT group compared with the normal group (Fig. 4, *B* and *C*). Treatment with high-dose edoxaban significantly reduced the numbers of CD68-positive macrophages and active NF-κB-positive cells in MCT-exposed rats (Fig. 4, *B* and *C*). Macrophages, PAECs, and PASMCs were observed as NF-κB-positive cells, with macrophages in particular showing a decrease in NF-κB-positive cells with high-dose edoxaban treatment (Supplemental Fig. S4, *A–C*).

The mRNA levels of interleukin-6 (*IL-6*), macrophage chemoattractant protein-1 (*MCP-1*), and plasminogen activator inhibitor-1 (*PAI-1*), which are the markers of inflammation, significantly increased in the MCT group, while those increases were inhibited significantly by treatment with high-dose edoxaban (Fig. 4, *D–F*).

Higher Levels of Factor X and PARs Gene Expression in PAH-PASMCs

The mRNA levels of *Factor X*, PAR_1, and PAR_2 in PAH-PASMCs were significantly and substantially higher than those seen in normal PASMCs (Fig. 5, *A–C*).

Effect of FXa on Cell Proliferation and Inflammatory Marker Expression in Normal PASMCs

Stimulation of normal PASMCs with 50 nM FXa resulted in a significant increase in BrdU incorporation. This increase was significantly suppressed to the control level by preadministration of 1 μM E5555 or 100 nM edoxaban, but not by 50 μM FSLLRY (Fig. 6*A*). The inhibitory effect of E5555 combined with FSLLRY was similar to that obtained by E5555 alone (Fig. 6*A*).

The levels of *IL-6*, *MCP-1*, and *PAI-1* mRNA expression increased significantly by FXa stimulation of normal PASMCs. Those increases were suppressed significantly by 1 μM E5555 or 100 nM edoxaban, but not by 50 μM FSLLRY (Fig. 6, *B–D*). The combination of E5555 and FSLLRY exhibited no additive suppressive effect compared with E5555 alone (Fig. 6, *B–D*).

In addition, these effects were not observed when PASMCs were not stimulated by FXa (Supplemental Fig. S5).

Effect of FXa on ERK1/2 Activity in Normal PASMCs

Stimulation of normal PASMCs with 50 nM FXa significantly increased the phosphorylation level of p44/42 extracellularly regulated kinases1/2 (ERK1/2), and that increase was significantly suppressed by 1 μM E5555 or 100 nM edoxaban, but not by 50 μM FSLLRY (Fig. 7). The combination of E5555 and FSLLRY did not show an additive effect compared with E5555 alone. In addition, we observed a trend of suppressed phosphorylated p-65 by edoxaban or E5555, although it was not statistically significant (Supplemental Fig. S6).

Effect of FXa on the Expression of Inflammatory Cytokines in Normal PASMCs Using PAR-1 Knockdown

We performed knockdown of PAR_1 in normal PASMCs using siRNA. The expression of *PAR-1* was significantly downregulated regardless of stimulation with FXa (Fig. 8*A*). Stimulation of normal PASMCs with 50 nM FXa resulted in a significant increase in BrdU incorporation. This increase was significantly suppressed by knockdown of PAR-1 (Fig. 8*B*). The levels of *IL-6*, *MCP-1*, and *PAI-1* mRNA expression increased significantly by FXa stimulation of normal PASMCs. Those increases were significantly downregulated by knockdown of PAR-1 (Fig. 8, *C–E*).

No Effect of Prolonged Treatment with Edoxaban on PH in SU5416/Hypoxia/Normoxia-Induced PH Rat Model

As an attempt to generalize the findings obtained from the MCT-exposed PH model, we produced the SU5416/hypoxia/normoxia-induced PH rat model and examined the therapeutic effect of edoxaban (Fig. 9*A*). There was no significant increase in plasma FXa activity at the end of 5 wk after SU5416 injection in SU5416/hypoxia/normoxia-induced PH rats compared with normal rats injected with PBS (Fig. 9*B*). RVSP and RV/(LV + S) ratio increased significantly in SU5416/hypoxia/normoxia-exposed PH model rats, and the increases were not affected by treatment with edoxaban (10 mg/kg/day) from the day of SU5416 injection to the end of *week 5* (Fig. 9, *C* and *D*).

DISCUSSION

The novel findings of the present study are: *1*) plasma FXa level was elevated in MCT-exposed rats; *2*) long-term treatment with edoxaban ameliorated the pathophysiological findings of PH, including vascular remodeling and inflammatory response in MCT-exposed rats; and *3*) FXa induced cell proliferation and inflammatory response in a PAR_1-dependent manner in human PASMCs. These results suggest

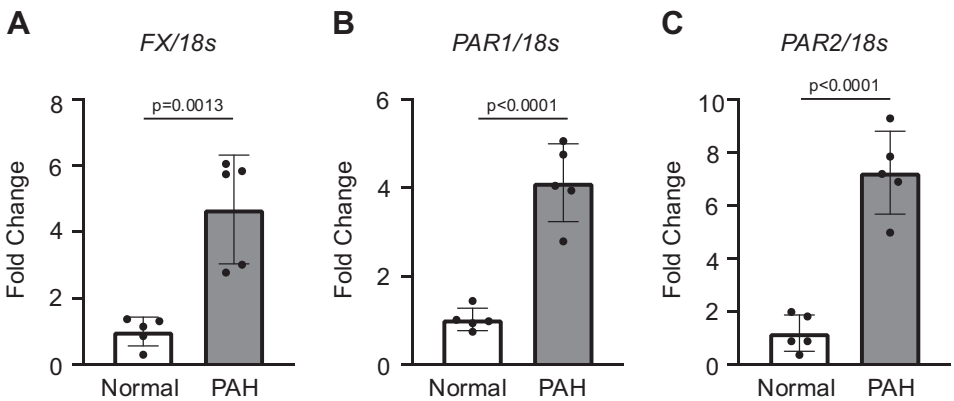


Figure 5. Quantification of factor X (FX) and proteinase-activated receptors (PAR) in cultured human pulmonary arterial smooth muscle cells (PASMCs) isolated from Non-PAH and PAH subjects. The expressions of mRNA levels of *FX* (*A*), PAR_1 (*B*), and PAR_2 (*C*) in PASMCs isolated from non-PAH patients with bronchogenic carcinoma (Normal PASMCs) and from patients with pulmonary arterial hypertension (PAH PASMCs) were measured by RT-PCR. Data are expressed as mean ± SD. $n = 5$, analyzed by paired *t* test.

Downloaded from journals.physiology.org/journal/ajplung (124.247.150.004) on July 27, 2025.

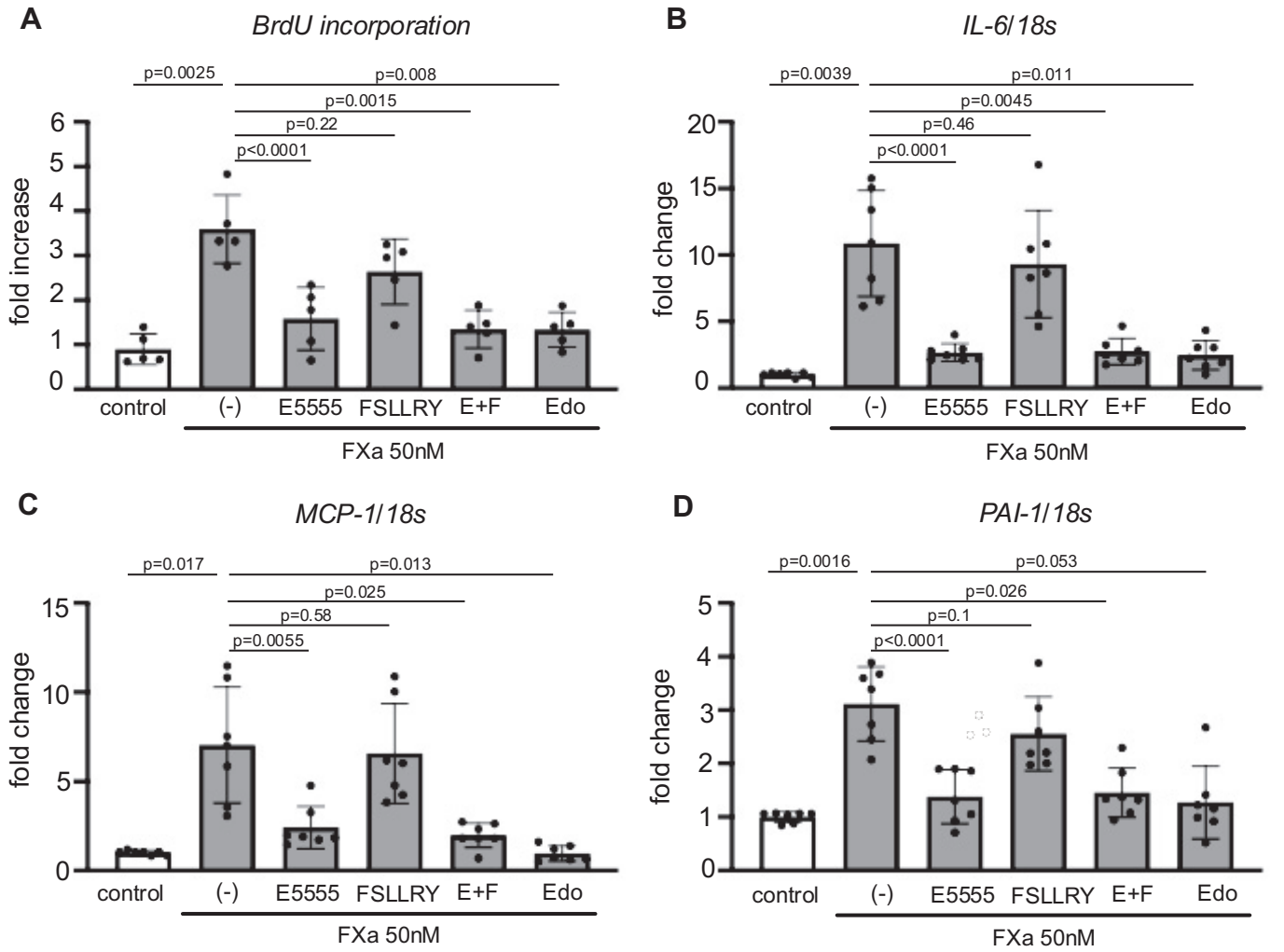


Figure 6. Mechanisms of activated factor X (Factor Xa) on proliferation and inflammatory signaling in cultured human pulmonary arterial smooth muscle cells (PASMCs) isolated from non-PAH subjects. Graphs show summaries of BrdU incorporation (*A*) and mRNA expression levels of *Il-6* (*B*), *MCP-1* (*C*), and *PAI-1* (*D*) without stimulation (control) and with stimulation by 50 nM FXa in the presence or absence of 1 μM E5555 (PAR_1 antagonist), 50 μM FSLLRY (PAR_2 antagonist), their combination (E + F), or 100 nM edoxaban (Edo) in PASMCs isolated from non-PAH patients with bronchogenic carcinoma (normal PASMCs). Data are expressed as mean ± SD. $n = 5–8$, analyzed by two-way repeated measures ANOVA. Il-6, interleukin-6; MCP-1, macrophage chemoattractant protein-1; PAI-1, plasminogen activator inhibitor-1.

that FXa inhibition is a potential novel therapeutic strategy for PAH.

FX is mainly produced by hepatocytes as a serine protease precursor located in the common pathway of the blood coagulation system and is activated by cleavage of an activating peptide by an upstream factor IXa. Activated FX (FXa) forms the prothrombinase complex together with factor Va and phospholipids, and mediates the conversion of prothrombin to thrombin (34). In addition to playing such a key role in blood coagulation, FXa is also involved in inflammatory responses by activating PAR_1 and/or PAR_2 outside blood vessels via extravascular leakage and extrahepatic synthesis (35). Edoxaban competitively and selectively inhibits the enzymatic activity of FXa in the blood vessels. For instance, FX is locally expressed and activates PARs in vascular smooth muscle cells within atherosclerotic plaques (11). In the present study, plasma FXa levels were significantly elevated in MCT-exposed rats compared with normal rats, and *FX* mRNA levels in PAH-PASMCs were higher than those seen in the normal PASMCs. Administration of FXa stimulated proliferation of normal PASMCs and upregulated the mRNA expression of proinflammatory cytokines. These cellular effects were abolished by not only by edoxaban but also by PAR_1 antagonist, but not by PAR_2 antagonist, although mRNA levels of both PAR_1 and PAR_2 in PAH-PASMCs were substantially higher than those in normal PASMCs. Moreover, knockdown of PAR_1 using siRNA downregulated the expression of proinflammatory cytokines by FXa stimulation to a comparable level of treatment with PAR_1 antagonist or edoxaban. These findings suggest that FXa-induced proliferative and proinflammatory effect on PASMCs is mediated by PAR_1 upregulation. These cellular effects of FXa may contribute to pulmonary vascular remodeling in PAH, at least in an experimental PH.

The pathological roles of PAR_1 and PAR_2 in experimental PH have been reported previously. Pharmacological antagonists and gene knockout of PAR_1 (13) and PAR_2 (12) prevented the development of experimental PH and ameliorated the

Downloaded from journals.physiology.org/journal/ajplung (124.247.150.004) on July 27, 2025.

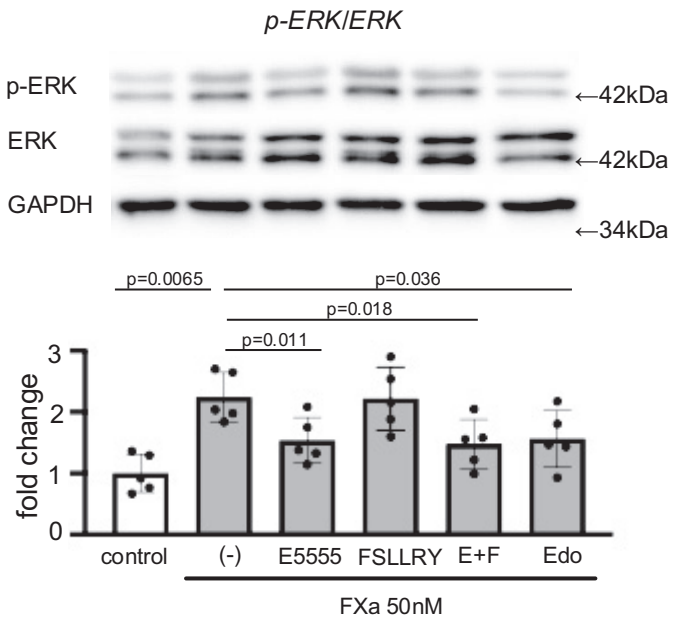


Figure 7. Effect of activated factor X (Factor Xa) on phosphorylation of ERK via proteinase-activated receptor (PAR) inhibitors in cultured human pulmonary arterial smooth muscle cells (PASMCs) isolated from Non-PAH subjects. Representative immunoblot images and summary of phosphorylated ER1/2 level without stimulation and with stimulation by 50 nM FXa in the presence or absence of 1 μM E5555 (PAR_1 antagonist), 50 μM FSLLRY (PAR_2 antagonist), their combination (E + F), or 100 nM edoxaban (Edo) in PASMCs isolated from non-PAH patients with bronchogenic carcinoma (normal PASMCs). Data are expressed as mean ± SD. $n = 5$, analyzed by one-way ANOVA followed by Bonferroni post hoc test. ERK, extracellularly regulated kinases; PAH, pulmonary arterial hypertension.

worsened hemodynamic parameters. We demonstrated that the mRNA level of PAR_1, but not the other isoforms of PARs, in pulmonary artery was significantly upregulated in MCT-exposed rats (13). Therefore, elevated PAR_1 levels are suggested to contribute to the development and the progression of experimental PH (13). However, the upstream factor that activates PAR_1 and contributes to the pathogenesis of PH remains to be elucidated. The proteinases that act as agonists for PAR_1 are not only limited to the coagulation-fibrinolysis factors such as thrombin, FVIIa, FXa, FXIa, FXIIa, activated protein C, and plasmin, but also include other proteinases such as metalloproteinase 1 and elastase (36–38). The findings of the present study suggest that FXa serves as PAR_1 agonist in the context of PH, although the contribution of thrombin cannot be ruled out because edoxaban inhibits not only PAR_1-mediated FXa activation but also conversion of prothrombin to thrombin, thereby masking the agonistic activity of thrombin to PAR_1.

The present study demonstrated that FXa upregulated the expression of some inflammatory markers via PAR_1 in normal PASMCs. Studies have shown that activation of PAR_1 phosphorylates ERK1/2 and NF-κB, thereby inducing cell proliferation through inflammatory cytokines such as IL-6 and MCP-1 in cultured VSMCs (39, 40). Similar mechanisms were also reported in MCT-exposed PH models, in which phosphorylation of ERK1/2 was associated with increases in IL-6, MCP-1, and PAI-1 levels (40) via activation of NF-κB, leading to cell proliferation in PASMCs (41–43). The present study demonstrated that FXa induced phosphorylation of ERK1/2 and increased mRNA levels of *IL-6*, *MCP-1*, and *PAI-1* in normal PASMCs. Thus, we speculate that ERK1/2 plays a key role as a downstream factor for the PAR_1-mediated inflammatory response and cell proliferation.

In this study, we have shown that the high dose of edoxaban ameliorated pulmonary vascular remodeling and inflammatory response in MCT-exposed rats. In the clinical settings, plasma concentrations of edoxaban during treatment with the clinical dose range (60–150 mg/day) correlate linearly with prothrombin times in healthy males (32, 44). The maximum prolongation of prothrombin time from baseline was 99% at the edoxaban dose of 60 mg and 128% at 90 mg. Considering that prothrombin times in rats treated with edoxaban at 3 and 10 mg/kg were 116% and 132%, respectively (45), both doses used in the present study are assumed to be within the clinically relevant range. Oral administration of edoxaban in rats has been shown to inhibit thrombosis at doses of 2.5 mg/kg and higher, and prolong bleeding time at doses of 20 mg/kg and higher (43). Considering that a low dose of edoxaban (3 mg/kg) did not ameliorate the increases in RVSP, TPRI, RV/(LV + S), and pulmonary vascular remodeling in MCT-exposed rats, whereas a high dose (10 mg/kg) effectively suppressed those parameters, the ameliorating effects observed with the high dose may not be related to inhibition of coagulation activity.

There are some controversies regarding the therapeutic effect of FXa inhibitor. One study demonstrated that rivaroxaban inhibited RVSP increase and RVH in an MCT-exposed PH model (46). This is consistent with our study; however, the authors did not demonstrate the specific mechanism how rivaroxaban lowered RVSP. Meanwhile, another study reported that chronic treatment with rivaroxaban had no significant therapeutic effect in hypoxia-induced PH mice, although the mice exhibited increased FXa protein levels in the lungs (47). One possible explanation for this discrepancy is the differences in the extent of activation of the coagulation system and the involvement of inflammation and inflammatory cytokines such as IL-6 in the pathophysiology between the two models. Accumulating evidence has shown that the perivascular inflammation plays an important role in the progression of pulmonary vascular remodeling in hypoxia-induced-PH mice. Ishibashi et al. (48) demonstrated that hypoxia-induced PH was suppressed in IL6 knockout mice. In addition, deletion of $CD4^+$ cell-specific gp130, a subunit of the IL6 receptor that facilitates JAK/STAT3 signaling, ameliorated hypoxia-induced PH. In which, hypoxia-induced increase of Th17 cells was suppressed by $CD4^+$ cell-specific gp130 deletion. These data suggest that IL6/gp130 signaling in $CD4^+$ cells plays a critical role in the pathogenesis of pulmonary vascular remodeling. Another study has shown that in *RAG1*$^{-/-}$ mice, mice that lack mature T and B cells, adoptive transfer of $CD4^+$ but not $CD8^+$ T cells developed hypoxia-induced PH (49). Moreover, *RAG1*$^{-/-}$ mice that received Th17 cells developed PH independent of hypoxia. Deletion of $CD4^+$ cells or inhibition of Th17 cells development prevented hypoxia-induced PH. Hashimoto-Kataoka et al. (50) demonstrated that IL-17 derived from Th17 cells stimulates production of IL-21, which promotes polarization of alveolar macrophage into M2 macrophage, inducing production of chemokines and cell proliferation. These data suggest that Th17 cells especially have an important role in the development of hypoxia-induced PH. In the present study, we

Downloaded from journals.physiology.org/journal/ajplung (124.247.150.004) on July 27, 2025.

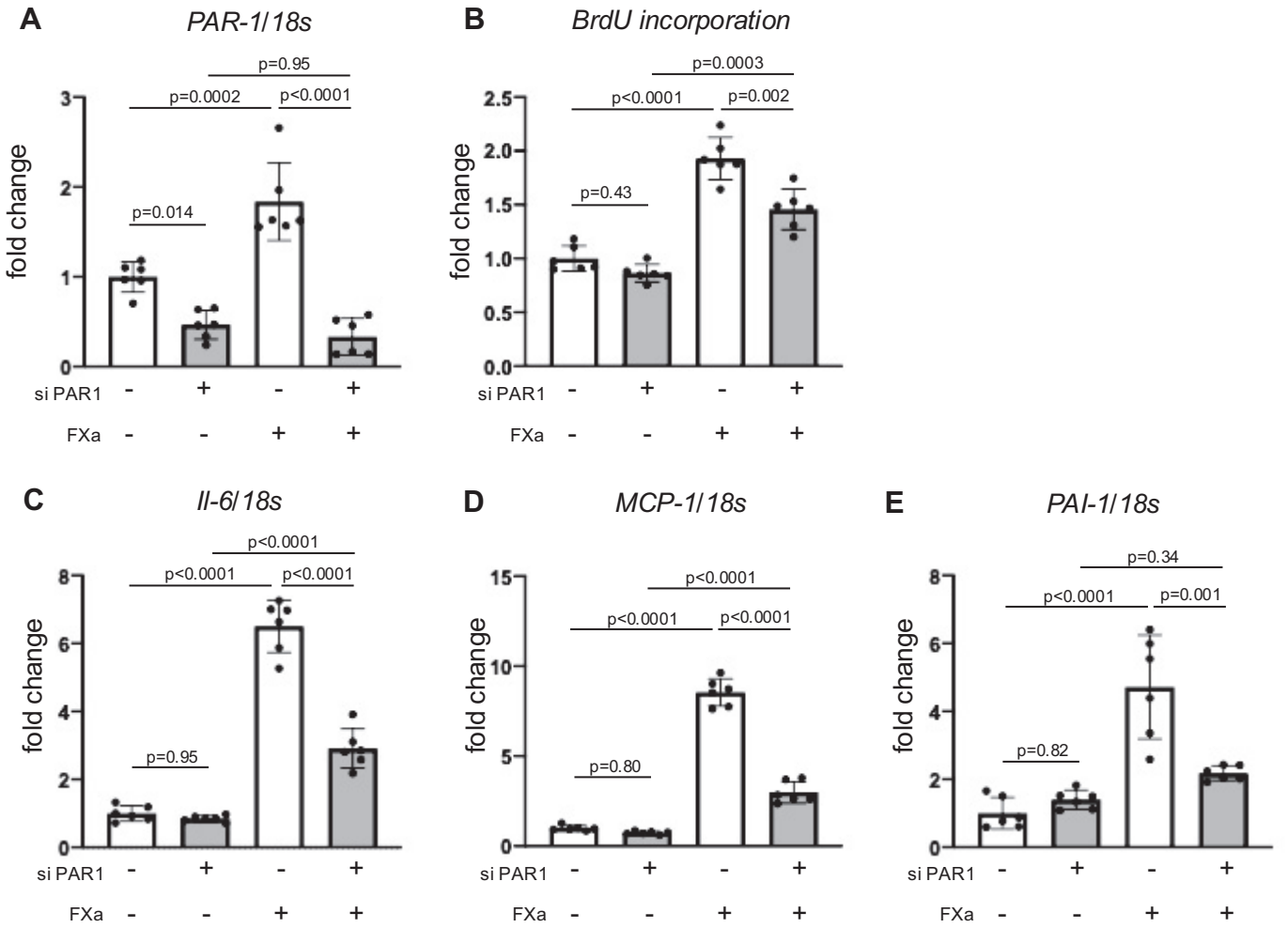


Figure 8. Mechanisms of activated factor X (Factor Xa) on inflammatory signaling in cultured human pulmonary arterial smooth muscle cells (PASMCs) isolated from non-PAH subjects. Graphs show summaries of mRNA expression levels of *PAR-1* (*A*), *Il-6* (*C*), *MCP-1* (*D*), and *PAI-1* (*E*) and BrdU incorporation (*B*) without stimulation (control) and with stimulation by 50 nM FXa in the presence or absence of PAR-1 gene knockdown in PASMCs isolated from non-PAH patients with bronchogenic carcinoma (normal PASMCs). siPAR1; siRNA targeted to PAR-1. Data are expressed as mean ± SD. $n = 6$, analyzed by two-way repeated measures ANOVA. Il-6, interleukin-6; MCP-1, macrophage chemoattractant protein-1; PAH, pulmonary arterial hypertension; PAI-1, plasminogen activator inhibitor-1.

have shown that edoxaban, the direct FXa inhibitor, not only inhibited coagulative pathway but also proinflammatory pathway via PAR1 suppression. This discrepancy between the response to FXa inhibition in MCT-exposed rats and hypoxia-induced mice may be partially explained by the predominancy of inflammatory pathway that involved in the pathogenesis of pulmonary remodeling in hypoxia-induced PH mice, while MCT-exposed rats are more heterogenous and diverse.

The involvement of inflammation has also been established in the SU5416/hypoxia/normoxia-induced PH rat model (22, 51). For example, the expression of IL-6 was markedly upregulated in the lung of 5-wk SU5416/hypoxia/normoxia-induced PH rats (22, 24, 52, 53). However, we observed no significant clinical therapeutic effect of edoxaban in SU5416/hypoxia/normoxia-induced PH rats. This negative result may be related to the finding of no difference in FXa and ERK1/2 activity between SU5416/hypoxia/normoxia-induced PH rats and normal rats, while we found increased expression of FXa and ERK1/2 in MCT-exposed rats. We speculate that the upstream mechanism of inflammation differs between the PH models, and therefore, the patients with PAH, which may infer the heterogeneous pathophysiology among patients with PAH. The need for personalized or precision medicine has recently emerged in the field of PH. Understanding the patient-specific pathophysiology based on deep molecular phenotyping and selecting the best-matched therapeutic strategy for each patient are now anticipated as the future direction (54, 55). When applying FXa inhibitor to the treatment of PAH, stratification of patients based on the activity of FXa and the state of inflammation is recommended. It should also be noted that the limitation of this experiment is that only male rats were used, and the possible sex difference in response to edoxaban cannot be ruled out. Moreover, although prevention protocol had effectively attenuated pulmonary vascular remodeling in this study, reversal protocol failed to attenuate pulmonary vascular remodeling. Which suggests that the antipulmonary vascular remodeling effect by edoxaban is

Downloaded from journals.physiology.org/journal/ajplung (124.247.150.004) on July 27, 2025.

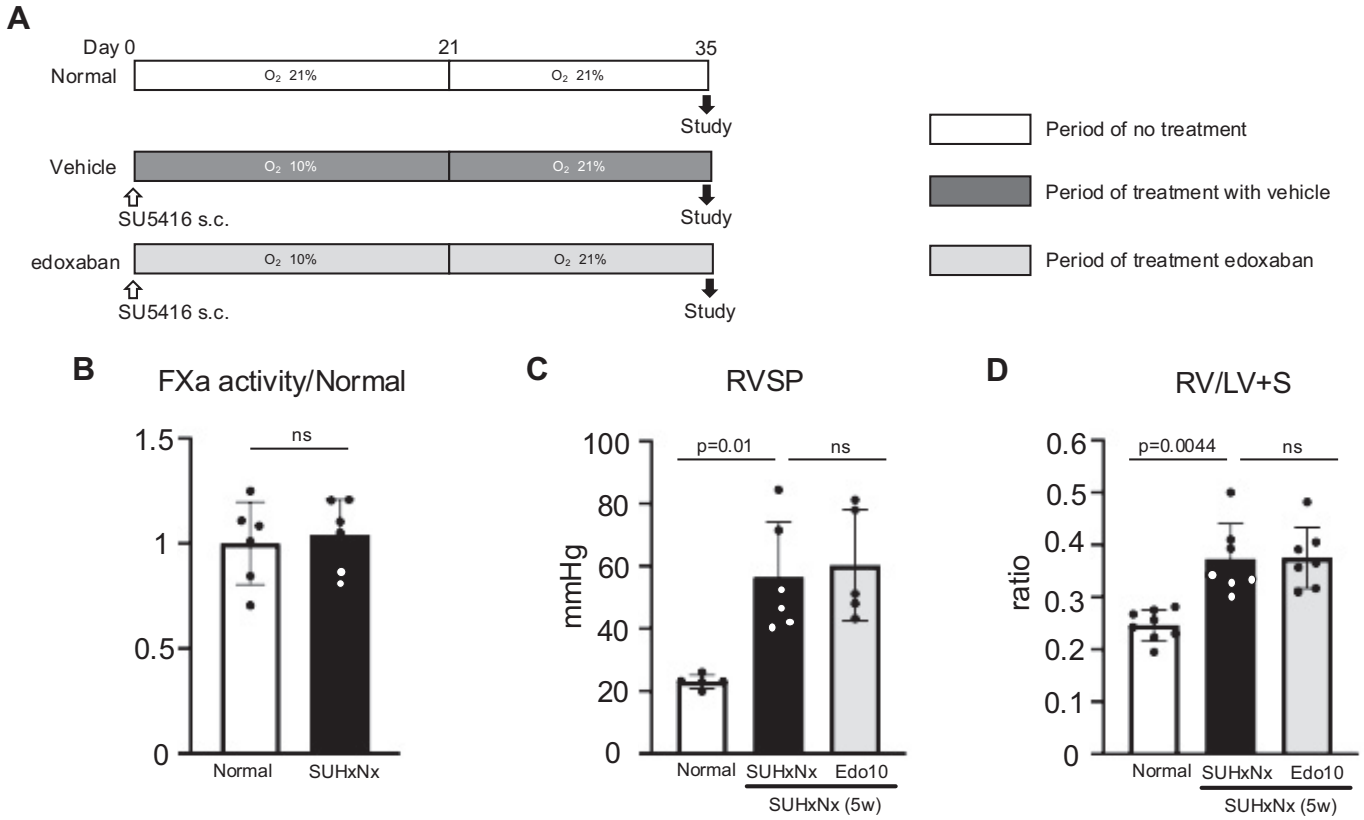


Figure 9. Effects of long-term treatment with edoxaban on hemodynamic parameters and right ventricular hypertrophy in SU5416/hypoxia/normoxia-induced rats. *A*: experimental protocol. Rats received a single subcutaneous injection of SU5416 (20 mg/kg) and were housed in hypoxic condition (10% O_2) for 3 wk and then in normoxic condition for 2 wk. Some SU5416/hypoxia/normoxia-induces rats were treated with edoxaban (10 mg/kg/day, by gavage) from *day 0* through to the end of *week 5* after SU5416 injection. Normal: normal rats injected with PBS instead of SU5416. SuHxNx: SU5416/hypoxia/normoxia-induced rats. *B*–*D*: summaries of activated factor X (FXa) activity in plasma (*B*), right ventricular systolic pressure (RVSP) (*C*), and right ventricular hypertrophy [RV/(LV + S): weight ratio of RV free wall to the sum of LV free wall and septum] (*D*) at the end of 5 wk after SU5416 injection. Data are expressed as mean ± SD. *B*: $n = 6$. Unpaired *t* test showed no significant difference. *C* and *D*: $n = 5$–8. *$P < 0.05$ and **$P < 0.01$ vs. Normal, analyzed by one-way ANOVA followed by Bonferroni post hoc test. PBS, phosphate-buffered saline.

effective in the early stage of the disease progression. Finally, in the cell experiment, there was a significant age difference between the normal and PAH PASMC, as shown in Table 2.

In conclusion, we demonstrated that chronic treatment with FXa inhibitor ameliorated NF-κB-IL-6-mediated perivascular inflammation in an MCT-exposed PH rat model, which is associated with augmented FXa activity. FXa may act on PASMCs, inducing cell proliferation and inflammatory response via upregulated PAR_1, thereby contributing to pulmonary vascular remodeling. Understanding the patient-specific pathophysiology, especially in terms of coagulation activity and inflammatory state, is a prerequisite for applying FXa-targeted therapy to the treatment of PAH.

DATA AVAILABILITY

Data will be made available upon reasonable request.

SUPPLEMENTAL MATERIAL

Supplemental Figs S1–S6: https://doi.org/10.6084/m9.figshare.29374289.

ACKNOWLEDGMENTS

We thank Akiko Ando for technical assistance. We appreciate the technical assistance from The Research Support Centre, Research Centre for Human Disease Modelling, Kyushu University Graduate School of Medical Sciences.

GRANTS

This work was supported by JSPS KAKENHI Grant (17K09591); and Japan Agency for Medical Research and Development (18ek0109371h0001).

DISCLOSURES

H. Tsutsui received honoraria from Daiichi Sankyo, Inc., Otsuka Pharmaceutical Co., Ltd., Takeda Pharmaceutical Co. Ltd., Mitsubishi Tanabe Pharma Corporation, Boehringer Ingelheim Japan, Inc., Novartis Pharma K.K., Bayer Yakuhin, Ltd., Bristol-Myers Squibb KK, and Astellas Pharma Inc.; and research funds from Actelion Pharmaceuticals Japan, Daiichi Sankyo, Co., Ltd., and Astellas Pharma Inc. K. Abe received a research grant from Mochida Pharmaceutical Co. and Actelion Pharmaceuticals Japan. None of the other authors has any conflicts of interest, financial or otherwise, to disclose.

Downloaded from journals.physiology.org/journal/ajplung (124.247.150.004) on July 27, 2025.

AUTHOR CONTRIBUTIONS

S.I., K.Y., K.H., and K.A. conceived and designed research; S.I., K.K., K.M., and R.I. performed experiments; S.I., K.K., K.Y., K.M., and R.I. analyzed data; S.I., K.K., K.Y., K.M., M.I., T.W., T.I., K.H., S.M., T.H., K.S., S.K., T.M., K.N., K.H., H.T., and K.A. interpreted results of experiments; S.I., K.K., and K.M. prepared figures; S.I., K.K., K.M., and K.H. drafted manuscript; S.I., K.K., K.Y., K.M., K.H., and K.A. edited and revised manuscript; S.I., K.K., K.Y., K.M., M.I., T.W., T.I., S.M., T.H., K.S., S.K., T.M., K.H., H.T., and K.A. approved final version of manuscript.

REFERENCES

1. **Humbert M**, **Guignabert C**, **Bonnet S**, **Dorfmüller P**, **Klinger JR**, **Nicolls MR**, **Olschewski AJ**, **Pullamsetti SS**, **Schermuly RT**, **Stenmark KR**, **Rabinovitch M.** Pathology and pathobiology of pulmonary hypertension: state of the art and research perspectives. *Eur Respir J* 53: 1801887, 2019. doi:10.1183/13993003.01887-2018.
2. **Humbert M**, **Sitbon O**, **Chaouat A**, **Bertocchi M**, **Habib G**, **Gressin V**, **Yaici A**, **Weitzenblum E**, **Cordier JF**, **Chabot F**, **Dromer C**, **Pison C**, **Reynaud-Gaubert M**, **Haloun A**, **Laurent M**, **Hachulla E**, **Simonneau G.** Pulmonary arterial hypertension in France - Results from a national registry. *Am J Respir Crit Care Med* 173: 1023–1030, 2006. doi:10.1164/rccm.200510-1668OC.
3. **Naeije R**, **Richter MJ**, **Rubin LJ.** The physiological basis of pulmonary arterial hypertension. *Eur Respir J* 59: 2102334, 2022. doi:10.1183/13993003.02334-2021.
4. **Pietra GG**, **Edwards WD**, **Kay JM**, **Rich S**, **Kernis J**, **Schloo B**, **Ayres SM**, **Bergofsky EH**, **Brundage BH**, **Detre KM.** Histopathology of primary pulmonary hypertension a qualitative and quantitative study of pulmonary blood vessels from 58 patients in the national heart, lung, and blood institute, primary pulmonary hypertension registry. *Circulation* 80: 1198–1206, 1989. doi:10.1161/01.cir.80.5.1198.
5. **White RJ**, **Meoli DF**, **Swarthout RF**, **Kallop DY**, **Galaria II**, **Harvey JL**, **Miller CM**, **Blaxall BC**, **Hall CM**, **Pierce RA**, **Cool CD**, **Taubman MB.** Plexiform-like lesions and increased tissue factor expression in a rat model of severe pulmonary arterial hypertension. *Am J Physiol Lung Cell Mol Physiol* 293: L583–L590, 2007. doi:10.1152/ajplung.00321.2006.
6. **Welsh CH**, **Hassell KL**, **Badesch DB**, **Kressin DC**, **Marlar RA.** Coagulation and fibrinolytic profiles in patients with severe pulmonary hypertension. *Article. Chest* 110: 710–717, 1996. doi:10.1378/chest.110.3.710.
7. **Eisenberg PR**, **Lucore C**, **Kaufman L**, **Sobel BE**, **Jaffe AS**, **Rich S.** Fibrinopeptide A levels indicative of pulmonary vascular thrombosis in patients with primary pulmonary hypertension. *Circulation* 82: 841–847, 1990. doi:10.1161/01.cir.82.3.841.
8. **Olsson KM**, **Delcroix M**, **Ghofrani HA**, **Tiede H**, **Huscher D**, **Speich R**, **Grünig E**, **Staehler G**, **Rosenkranz S**, **Halank M**, **Held M**, **Lange TJ**, **Behr J**, **Klose H**, **Claussen M**, **Ewert R**, **Opitz CF**, **Vizza CD**, **Scelsi L**, **Vonk-Noordegraaf A**, **Kaemmerer H**, **Gibbs JSR**, **Coghlan G**, **Pepke-Zaba J**, **Schulz U**, **Gorenflo M**, **Pittrow D**, **Hoeper MM.** Anticoagulation and survival in pulmonary arterial hypertension. *Circulation* 129: 57–65, 2014. doi:10.1161/circulationaha.113.004526.
9. **Tournier A**, **Wahl D**, **Chaouat A**, **Max JP**, **Regnault V**, **Lecompte T**, **Chabot F.** Calibrated automated thrombography demonstrates hypercoagulability in patients with idiopathic pulmonary arterial hypertension. *Thromb Res* 126: E418–E422, 2010. doi:10.1016/j.thromres.2010.08.020.
10. **Hara T**, **Fukuda D**, **Tanaka K**, **Higashikuni Y**, **Hirata Y**, **Yagi S**, **Soeki T**, **Shimabukuro M**, **Sata M.** Inhibition of activated factor X by rivaroxaban attenuates neointima formation after wire-mediated vascular injury. *Eur J Pharmacol* 820: 222–228, 2018. doi:10.1016/j.ejphar.2017.12.037.
11. **Sanada F**, **Muratsu J**, **Otsu R**, **Shimizu H**, **Koibuchi N**, **Uchida K**, **Taniyama Y**, **Yoshimura S**, **Rakugi H**, **Morishita R.** Local production of activated factor x in atherosclerotic plaque induced vascular smooth muscle cell senescence. *Sci Rep* 7: 17172, 2017. doi:10.1038/s41598-017-17508-6.
12. **Kwapiszewska G**, **Markart P**, **Dahal BK**, **Kojonazarov B**, **Marsh LM**, **Schermuly RT**, **Taube C**, **Meinhardt A**, **Ghofrani HA**, **Steinhoff M**, **Seeger W**, **Preissner KT**, **Olschewski A**, **Weissmann N**, **Wygrecka M.** PAR-2 inhibition reverses experimental pulmonary hypertension. *Circ Res* 110: 1179–1191, 2012. doi:10.1161/CIRCRESAHA.111.257568.
13. **Kuwabara Y**, **Tanaka-Ishikawa M**, **Abe K**, **Hirano M**, **Hirooka Y**, **Tsutsui H**, **Sunagawa K**, **Hirano K.** Proteinase-activated receptor 1 antagonism ameliorates experimental pulmonary hypertension. *Cardiovasc Res* 115: 1357–1368, 2019. doi:10.1093/cvr/cvy284.
14. **Kolettis T**, **Vlahos AP**, **Louka M**, **Hatzistergos KE**, **Baltogiannis GG**, **Agelaki MM**, **Mitsi A**, **Malamou-Mitsi V.** Characterisation of a rat model of pulmonary arterial hypertension. *Hellenic J Cardiol* 48: 206–210, 2007. doi:10.3791/53335.
15. **Bal E**, **Ilgin S**, **Atli O**, **Ergun B**, **Sirmagul B.** The effects of gender difference on monocrotaline-induced pulmonary hypertension in rats. *Hum Exp Toxicol* 32: 766–774, 2013. doi:10.1177/0960327113477874.
16. **Scotton CJ**, **Krupiczojc MA**, **Königshoff M**, **Mercer PF**, **Lee YC**, **Kaminski N**, **Morser J**, **Post JM**, **Maher TM**, **Nicholson AG**, **Moffatt JD**, **Laurent GJ**, **Derian CK**, **Eickelberg O**, **Chambers RC.** Increased local expression of coagulation factor X contributes to the fibrotic response in human and murine lung injury. *J Clin Invest* 119: 2550–2563, 2009. doi:10.1172/jci33288.
17. **Oe Y**, **Hayashi S**, **Fushima T**, **Sato E**, **Kisu K**, **Sato H**, **Ito S**, **Takahashi N.** Coagulation factor xa and protease-activated receptor 2 as novel therapeutic targets for diabetic nephropathy. *Arterioscler Thromb Vasc Biol* 36: 1525–1533, 2016. doi:10.1161/ATVBAHA.116.307883.
18. **Abe K**, **Toba M**, **Alzoubi A**, **Ito M**, **Fagan KA**, **Cool CD**, **Voelkel NF**, **McMurtry IF**, **Oka M.** Formation of plexiform lesions in experimental severe pulmonary arterial hypertension. *Circulation* 121: 2747–2754, 2010. doi:10.1161/circulationaha.109.927681.
19. **Toba M**, **Alzoubi A**, **O'Neill KD**, **Gairhe S**, **Matsumoto Y**, **Oshima K**, **Abe K**, **Oka M**, **McMurtry IF.** Temporal hemodynamic and histological progression in Sugen5416/hypoxia/normoxia-exposed pulmonary arterial hypertensive rats. *Am J Physiol Heart Circ Physiol* 306: H243–H250, 2014. doi:10.1152/ajpheart.00728.2013.
20. **Schwenke DO**, **Pearson JT**, **Sonobe T**, **Ishibashi-Ueda H**, **Shimouchi A**, **Kangawa K**, **Umetani K**, **Shirai M.** Role of Rho-kinase signaling and endothelial dysfunction in modulating blood flow distribution in pulmonary hypertension. *J Appl Physiol (1985)* 110: 901–908, 2011. doi:10.1152/japplphysiol.01318.2010.
21. **Guignabert C**, **Phan C**, **Seferian A**, **Huertas A**, **Tu L**, **Thuillet R**, **Sattler C**, **Le Hiress M**, **Tamura Y**, **Jutant EM**, **Chaumais MC**, **Bouchet S**, **Manéglier B**, **Molimard M**, **Rousselot P**, **Sitbon O**, **Simonneau G**, **Montani D**, **Humbert M.** Dasatinib induces lung vascular toxicity and predisposes to pulmonary hypertension. *J Clin Invest* 126: 3207–3218, 2016. doi:10.1172/JCI86249.
22. **Tamura Y**, **Phan C**, **Tu L**, **Le Hiress M**, **Thuillet R**, **Jutant E-M**, **Fadel E**, **Savale L**, **Huertas A**, **Humbert M**, **Guignabert C.** Ectopic upregulation of membrane-bound IL6R drives vascular remodeling in pulmonary arterial hypertension. *J Clin Invest* 128: 1956–1970, 2018. doi:10.1172/jci96462.
23. **Garcia-Martinez I**, **Santoro N**, **Chen YL**, **Hoque R**, **Ouyang XS**, **Caprio S**, **Shlomchik MJ**, **Coffman RL**, **Candia A**, **Mehal WZ.** Hepatocyte mitochondrial DNA drives nonalcoholic steatohepatitis by activation of TLR9. *J Clin Invest* 126: 859–864, 2016. doi:10.1172/jci83885.
24. **Abe K**, **Shinoda M**, **Tanaka M**, **Kuwabara Y**, **Yoshida K**, **Hirooka Y**, **McMurtry IF**, **Oka M**, **Sunagawa K.** Haemodynamic unloading reverses occlusive vascular lesions in severe pulmonary hypertension. *Cardiovasc Res* 111: 16–25, 2016. doi:10.1093/cvr/cvw070.
25. **Ishikawa T**, **Abe K**, **Takana-Ishikawa M**, **Yoshida K**, **Watanabe T**, **Imakiire S**, **Hosokawa K**, **Hirano M**, **Hirano K**, **Tsutsui H.** Chronic inhibition of toll-like receptor 9 ameliorates pulmonary hypertension in rats. *J Am Heart Assoc* 10: e019247, 2021. doi:10.1161/jaha.120.019247.
26. **Tanaka M**, **Abe K**, **Oka M**, **Saku K**, **Yoshida K**, **Ishikawa T**, **McMurtry IF**, **Sunagawa K**, **Hoka S**, **Tsutsui H.** Inhibition of nitric oxide synthase unmasks vigorous vasoconstriction in established pulmonary arterial hypertension. *Physiol Rep* 5: e13537, 2017. doi:10.14814/phy2.13537.
27. **Wu F**, **Zhang YT**, **Teng F**, **Li HH**, **Guo SB.** S100a8/a9 contributes to sepsis-induced cardiomyopathy by activating ERK1/2-Drp1-mediated mitochondrial fission and respiratory dysfunction. *Int Immunopharmacol* 115: 109716, 2023. doi:10.1016/j.intimp.2023.109716.

Downloaded from journals.physiology.org/journal/ajplung (124.247.150.004) on July 27, 2025.

28. **Nakamura K**, **Shimizu J**, **Kataoka N**, **Hashimoto K**, **Ikeda T**, **Fujio H**, **Ohta-Ogo K**, **Ogawa A**, **Miura A**, **Mohri S**, **Nagase S**, **Morita H**, **Kusano KF**, **Date H**, **Matsubara H**, **Mochizuki S**, **Hashimoto K**, **Kajiya F**, **Ohe T.** Altered nano/micro-order elasticity of pulmonary artery smooth muscle cells of patients with idiopathic pulmonary arterial hypertension. *Int J Cardiol* 140: 102–107, 2010. doi:10.1016/j.ijcard.2008.11.022.
29. **Wei LP**, **Yu XF**, **Shi HY**, **Zhang B**, **Lian MM**, **Li J**, **Shen TT**, **Xing Y**, **Zhu DL.** 15-PGDH/15-KETE plays a role in hypoxia-induced pulmonary vascular remodeling through ERK1/2-dependent PAR-2 pathway. *Cell Signal* 26: 1476–1488, 2014. doi:10.1016/j.cellsig.2014.03.008.
30. **Morrison SA**, **Jesty J.** Tissue factor-dependent activation of tritium-labeled factor IX and factor x in human plasma. *Blood* 63: 1338–1347, 1984.
31. **Mitsui S**, **Oe Y**, **Sekimoto A**, **Sato E**, **Hashizume Y**, **Yamakage S**, **Kumakura S**, **Sato H**, **Ito S**, **Takahashi N.** Dual blockade of protease-activated receptor 1 and 2 additively ameliorates diabetic kidney disease. *Am J Physiol Renal Physiol* 318: F1067–F1073, 2020. doi:10.1152/ajprenal.00595.2019.
32. **Furugohri T**, **Isobe K**, **Honda Y**, **Kamisato-Matsumoto C**, **Sugiyama N**, **Nagahara T**, **Morishima Y**, **Shibano T.** DU-176b, a potent and orally active factor Xa inhibitor: in vitro and in vivo pharmacological profiles. *J Thromb Haemost* 6: 1542–1549, 2008. doi:10.1111/j.1538-7836.2008.03064.x.
33. **Ishikita A**, **Matsushima S**, **Ikeda S**, **Okabe K**, **Nishimura R**, **Tadokoro T**, **Enzan N**, **Yamamoto T**, **Sada M**, **Tsutsui Y**, **Miyake R**, **Ikeda M**, **Ide T**, **Kinugawa S**, **Tsutsui H.** GFAT2 mediates cardiac hypertrophy through HBP-O-GlcNAcylation-Akt pathway. *iScience* 24: 103517, 2021. doi:10.1016/j.isci.2021.103517.
34. **Camire RM.** Blood coagulation factor X: molecular biology, inherited disease, and engineered therapeutics. *J Thromb Thrombolysis* 52: 383–390, 2021. doi:10.1007/s11239-021-02456-w.
35. **Ruf W.** Roles of factor Xa beyond coagulation. *J Thromb Thrombolysis* 52: 391–396, 2021. doi:10.1007/s11239-021-02458-8.
36. **Peach CJ**, **Edgington-Mitchell LE**, **Bunnett NW**, **Schmidt BL.** Protease-activated receptors in health and disease. *Physiol Rev* 103: 717–785, 2023. doi:10.1152/physrev.00044.2021.
37. **Liu W**, **Hashimoto T**, **Yamashita T**, **Hirano K.** Coagulation factor XI induces Ca. *Am J Physiol Cell Physiol* 316: C377–C392, 2019. doi:10.1152/ajpcell.00426.2018.
38. **Jaffar J**, **McMillan L**, **Wilson N**, **Panousis C**, **Hardy C**, **Cho HJ**, **Symons K**, **Glaspole I**, **Westall G**, **Wong M.** Coagulation factor-XII induces interleukin-6 by primary lung fibroblasts: a role in idiopathic pulmonary fibrosis? *Am J Physiol Lung Cell Mol Physiol* 322: L258–L272, 2022. doi:10.1152/ajplung.00165.2021.
39. **Arisato T**, **Sarker KP**, **Kawahara K**, **Nakata M**, **Hashiguchi T**, **Osame M**, **Kitajima I**, **Maruyama I.** The agonist of the protease-activated receptor-1 (PAR) but not PAR3 mimics thrombin-induced vascular endothelial growth factor release in human vascular smooth muscle cells. *Cell Mol Life Sci* 60: 1716–1724, 2003. doi:10.1007/s00018-003-3140-6.
40. **Nakajima T**, **Kitajima I**, **Shin H**, **Takasaki I**, **Shigeta K**, **Abeyama K**, **Yamashita Y**, **Tokioka T**, **Soejima Y**, **Maruyama I.** Involvement of nf-kappa-b activation in thrombin-induced human vascular smooth muscle cell proliferation. *Biochem Biophys Res Commun* 204: 950–958, 1994. doi:10.1006/bbrc.1994.2552.
41. **Diebold I**, **Djordjevic T**, **Hess J**, **Görlach A.** Rac-1 promotes pulmonary artery smooth muscle cell proliferation by upregulation of plasminogen activator inhibitor-1: role of NFkappa B-dependent hypoxia-inducible factor-1 alpha transcription. *Thromb Haemost* 100: 1021–1028, 2008. doi:10.1160/TH08-07-0473.
42. **Rosenkranz AC**, **Rauch BH**, **Freidel K**, **Schrör K.** Regulation of protease-activated receptor-1 by vasodilatory prostaglandins via NFAT. *Cardiovasc Res* 83: 778–784, 2009. doi:10.1093/cvr/cvp163.
43. **Steiner MK**, **Syrkina OL**, **Kolliputi N**, **Mark EJ**, **Hales CA**, **Waxman AB.** Interleukin-6 overexpression induces pulmonary hypertension. *Circ Res* 104: 236–244, 2009. doi:10.1161/circresaha.108.182014.
44. **Morishima Y**, **Honda Y**, **Kamisato C**, **Tsuji N**, **Kita A**, **Edo N**, **Shibano T.** Comparison of antithrombotic and haemorrhagic effects of edoxaban, an oral direct factor Xa inhibitor, with warfarin and enoxaparin in rats. *Thromb Res* 130: 514–519, 2012. doi:10.1016/j.thromres.2012.05.008.
45. **Ogata K**, **Mendell-Harary J**, **Tachibana M**, **Masumoto H**, **Oguma T**, **Kojima M**, **Kunitada S.** Clinical safety, tolerability, pharmacokinetics, and pharmacodynamics of the novel factor Xa inhibitor edoxaban in healthy volunteers. *J Clin Pharmacol* 50: 743–753, 2010. doi:10.1177/0091270009351883.
46. **Delbeck M**, **Nickel KF**, **Perzborn E**, **Ellinghaus P**, **Strassburger J**, **Kast R**, **Laux V**, **Schäfer S**, **Schermuly RT**, **von Degenfeld G.** A role for coagulation factor Xa in experimental pulmonary arterial hypertension. *Cardiovasc Res* 92: 159–168, 2011. doi:10.1093/cvr/cvr168.
47. **Joseph C**, **Berghausen EM**, **Behringer A**, **Rauch B**, **Ten Freyhaus H**, **Gnatzy-Feik LL**, **Krause M**, **Wong DWL**, **Boor P**, **Baldus S**, **Vantler M**, **Rosenkranz S.** Coagulation-independent effects of thrombin and Factor Xa: role of protease-activated receptors in pulmonary hypertension. *Cardiovasc Res* 118: 3225–3238, 2022. doi:10.1093/cvr/cvac004.
48. **Ishibashi T**, **Inagaki T**, **Okazawa M**, **Yamagishi A**, **Ohta-Ogo K**, **Asano R**, **Masaki T**, **Kotani Y**, **Ding X**, **Chikaishi-Kirino T**, **Maedera N**, **Shirai M**, **Hatakeyama K**, **Kubota Y**, **Kishimoto T**, **Nakaoka Y.** IL-6/gp130 signaling in $CD4^+$ T cells drives the pathogenesis of pulmonary hypertension. *Proc Natl Acad Sci USA* 121: e2315123121, 2024. doi:10.1073/pnas.2315123121.
49. **Maston LD**, **Jones DT**, **Giermakowska W**, **Howard TA**, **Cannon JL**, **Wang W**, **Wei Y**, **Xuan W**, **Resta TC**, **Gonzalez Bosc LV.** Central role of T helper 17 cells in chronic hypoxia-induced pulmonary hypertension. *Am J Physiol Lung Cell Mol Physiol* 312: L609–L624, 2017. doi:10.1152/ajplung.00531.2016.
50. **Kataoka T**, **Hosen N**, **Sonobe T**, **Arita Y**, **Yasui T**, **Masaki T**, **Minami M**, **Inagaki T**, **Miyagawa S**, **Sawa Y**, **Murakami M**, **Kumanogoh A**, **Yamauchi-Takihara K**, **Okumura M**, **Kishimoto T**, **Komuro I**, **Shirai M**, **Sakata Y**, **Nakaoka Y.** Interleukin-6/interleukin-21 signaling axis is critical in the pathogenesis of pulmonary arterial hypertension. *Proc Natl Acad Sci USA* 112: E2677–E2686, 2015. doi:10.1073/pnas.1424774112.
51. **Mizuno S**, **Farkas L**, **Al Husseini A**, **Farkas D**, **Gomez-Arroyo J**, **Kraskauskas D**, **Nicolls MR**, **Cool CD**, **Bogaard HJ**, **Voelkel NF.** Severe pulmonary arterial hypertension induced by su5416 and ovalbumin immunization. *Am J Respir Cell Mol Biol* 47: 679–687, 2012. doi:10.1165/rcmb.2012-0077oc.
52. **Frump AL**, **Goss KN**, **Vayl A**, **Albrecht M**, **Fisher A**, **Tursunova R**, **Fierst J**, **Whitson J**, **Cucci AR**, **Brown MB**, **Lahm T.** Estradiol improves right ventricular function in rats with severe angioproliferative pulmonary hypertension: effects of endogenous and exogenous sex hormones. *Am J Physiol Lung Cell Mol Physiol* 308: L873–L890, 2015. doi:10.1152/ajplung.00006.2015.
53. **Yoshida K**, **Saku K**, **Kamada K**, **Abe K**, **Tanaka-Ishikawa M**, **Tohyama T**, **Nishikawa T**, **Kishi T**, **Sunagawa K**, **Tsutsui H.** Electrical vagal nerve stimulation ameliorates pulmonary vascular remodeling and improves survival in rats with severe pulmonary arterial hypertension. *JACC Basic Transl Sci* 3: 657–671, 2018. doi:10.1016/j.jacbts.2018.07.007.
54. **Wilkins MR.** Personalized medicine for pulmonary hypertension: the future management of pulmonary hypertension requires a new taxonomy. *Clin Chest Med* 42: 207–216, 2021. doi:10.1016/j.ccm.2020.10.004.
55. **Hemnes AR**, **Leopold JA**, **Radeva MK**, **Beck GJ**, **Abidov A**, **Aldred MA**, **et al.** Clinical characteristics and transplant-free survival across the spectrum of pulmonary vascular disease. *J Am Coll Cardiol* 80: 697–718, 2022. doi:10.1016/j.jacc.2022.05.038.

Downloaded from journals.physiology.org/journal/ajplung (124.247.150.004) on July 27, 2025.